

Numerical modelling of the Earth's ionosphere F region

P A Ostanin¹, D V Kulyamin², V P Dymnikov³

¹ Moscow Institute of Physics and Technology (MIPT SU), Institutskiy per., 9, Dolgoprudny, Moscow Region, 141701, Russian Federation

² Lomonosov Moscow State University, Research Computing Center (RCC), Leninskiye gory, 1, Moscow, 118991, Russian Federation

³ Institute of Numerical Mathematics of the Russian Academy of Sciences (INM RAS) Gubkin str., 8, Moscow, 118333, Russia

E-mail: ostanin.pavel@phystech.edu

Abstract. This paper presents the first version of a new INM RAS Earth's ionosphere F region dynamical model. A complete set of model equations is formulated taking into account all the key physical processes that form the global state of the ionospheric F region (plasma chemistry, ambipolar diffusion, wind transport, drift across magnetic lines). For the numerical solution, a splitting method based on the physical processes and geometric directions is proposed. The first stage of splitting in a quasi-two-dimensional approximation setting with a projection of ambipolar diffusion on the vertical direction is considered. It is numerically implemented stepwise using various difference schemes for three separate model formulations (taking into account diffusion only along the vertical direction, considering a realistic direction of diffusion along the magnetic field excluding and including a mixed derivative term). The applicability, efficiency, conservation, and monotonicity of these numerical methods are analyzed. The first numerical experiments show convergence of the numerical solution to a stationary vertical profile specific to the F region. The greatest consistency with the observed profiles is obtained in the mid-latitudes. Using the thus constructed model it is shown that the electron density profile is most sensitive to the neutral temperature and ionization level with qualitatively different structures of the corresponding modes of variability.

1. Introduction

This paper addresses the fundamental problem of describing and predicting the mean global state and variability of the Earth's ionosphere, as well as the physical mechanism of its formation, by numerical modeling of the F region with particular attention to the construction of efficient numerical methods and algorithms of their implementation. This work lies within the framework of a wider research direction currently being carried out at the Institute of Numerical Mathematics of the Russian Academy of Sciences (INM RAS), which is connected with the construction of upper atmosphere global models as parts of a comprehensive unified INM RAS Earth's system model. It aims at the development of a new consistent high-level coupled ionosphere-thermosphere dynamical numerical model.

The main objective of this paper is to present a numerical implementation and first results of numerical experiments with a new INM RAS Earth's ionosphere dynamical model. Primary attention is paid to an analysis of the model equations and a detailed description of the



numerical methods with investigation of their properties and efficiency. Further perspective is the integration of this model into a developed INM RAS thermosphere global dynamical model [1] in order to create the first version of a consistent upper atmosphere coupled model and couple it with INM RAS models of lower atmosphere and ionosphere layers [2].

The importance of this problem is caused by recently increased practical interest in the research and forecasting of space weather, which is connected with the specific role of ionospheric conditions for global radio and satellite communication, as well as for the whole space industry. The state of thermosphere-ionosphere system determines the characteristics of the low-orbit satellite motion and the conditions for radio signal propagation (which ensures stable operation of distant communications and global navigation systems).

At the same time, there is a certain disconnection nowadays between the traditional semi-empirical approach to the upper atmosphere study and the high-tech numerical modeling methods successfully applied to weather and climate change forecasting. The problem of describing the Earth's ionosphere characteristics is traditionally solved by processing the available experimental data and the construction of empirical models. These models of upper atmosphere basically describe the climatological state and for the most part do not take into account the variability of the environment caused by both external and internal factors (such as significant perturbations of radiation and electromagnetic fields, nonlinear wave processes in the thermosphere and ionosphere, etc.). In the meantime, these models are widely used to solve important practical problems. The most known examples of such reference models are IRI, SIMP, GOST [3-5] and others.

It is also important to note that the upper atmosphere numerical models are smaller in number and less developed in comparison with the modern weather forecast and climate models which take into account the lower atmosphere. The most advanced ionospheric models are developed mainly at global national centers and consortiums of various institutions; examples are the advanced coupled models of the thermosphere and ionosphere, such as the large American National Center for Atmospheric Research (NCAR) models TIEGCM, TIEM-GCM [6,7]; British UCL CTIP-CMAT [8]; domestic models UAM [9], GCM-TIP [10]. Modern ionospheric models developed in the past few decades (such as GAIM (originally TDIM) [11], or a Russian CAO assimilative ionospheric model [12]) utilize approaches based on data assimilation systems (using GPS network data). Mathematically, a common disadvantage of today's upper atmospheric models is that their basic versions were developed in the 1980-1990s under severe restrictions associated with the relatively poor performance of the computer facilities at that time, as well as the insufficient efficiency of the numerical methods. These models essentially use the generalized features of the mean ionospheric structure (the exponential character of the neutral components distribution in the radial direction, the predominant propagation of charged particles along the magnetic field lines, etc.), and do not take into account the latest research data of the thermosphere and ionosphere. Thus, creating a substantially new methodology for modeling and predicting the global state and variability of the ionosphere-thermosphere system based on the successful experience of INM RAS in Earth's climate modeling, research, and numerical forecasting is very important.

In this work the first version of the developed INM RAS ionosphere F region global dynamical model is presented. A description of the complete problem statement, model physical foundations, and solved equations is contained in the second section of the paper. The third chapter is devoted to a description of a stepwise methodology for this model implementation and a detailed analysis of the numerical methods used. The fourth section presents the results of numerical experiments. The fifth chapter contains a final discussion of the results and plans for further work.

2. Ionosphere F region model

2.1. Problem formulation

The first version of the dynamical ionosphere model is based on the following assumptions: considering only the F region, photochemical dominance of atomic oxygen O ionization and O^+ ion recombination with major air components and, thereby, a single-ion assumption, plasma quasineutrality (equality of the electron and ion concentrations $n_e = n_i = n$), a simultaneous motion of the electrons and ions along magnetic field lines in ambipolar diffusion, electromagnetic drift dominance, a dipole Earth's magnetic field with coincidence of the magnetic and geographic poles. We considered an altitude region of 100 – 500 km, which also includes lower ionospheric layers (E region). However, in the first version of the dynamical ionosphere model the emphasis is on the formation of the F layer and the role of dynamic processes. In this case the physical processes of the lower layers are not reproduced by this model [13]. The lower boundary is formally taken far from the electron concentration maximum in order to reduce its impact on the calculated distribution. A detailed consideration of D and E ionosphere layers in a unified atmosphere INM RAS model is implemented in a separate module by virtue of the dominance of photochemistry processes in these regions.

The main equation of the model is the continuity equation for the electron concentration n :

$$\frac{\partial n}{\partial t} + \text{div}(n\vec{u}) = P - kn, \quad (1)$$

where \vec{u} is the plasma transfer velocity connected with diffusion, neutral wind and electromagnetic drift. The velocity can be calculated [13], and equation (1) can be rewritten in the following form:

$$\frac{\partial n}{\partial t} = P - kn - \text{div}(n\vec{u}_{n\parallel}) - \text{div}\left(n\frac{[\vec{E} \times \vec{B}]}{B^2}\right) + \text{div}\left(D\left[\vec{\nabla}_{\parallel}n + n\frac{1}{T_p}\vec{\nabla}_{\parallel}T_p - \frac{nm_i}{2kT_p}\vec{g}_{\parallel}\right]\right). \quad (2)$$

In this equation $D = \frac{2kT_p}{m_i\nu_{in}}$ is the ambipolar diffusion coefficient, $\nu_{in} \approx 10^{-14} \cdot \sqrt{\frac{1}{2}(T_i + T_n)} \cdot n_O$ [s⁻¹] is the frequency of O^+ collisions with neutrals, m_i is the ion atom mass, \vec{g} is the gravitational field of the Earth, \vec{E} is the external electric field (magnetospheric convection, etc.), \vec{B} is the Earth's magnetic field, \vec{u}_n is the neutral field velocity, T_n is the neutral temperature, $T_p = \frac{1}{2}(T_e + T_i)$ is the mean of the electron and ion temperatures, and the index \parallel indicates projection on the magnetic field lines [13]. The components in the right hand side stand for the ionization process from O to O^+ and for the recombination loss. In this first version of the model only fixed daytime values of P and k are used: $P = 4 \cdot 10^{-7} \cdot n_O(z)$ [s⁻¹], $k = 1,2 \cdot 10^{-12} \cdot n_{N_2}(z) + 2,1 \cdot 10^{-11} \cdot n_{O_2}(z)$ [s⁻¹]. In the expressions above n_O, n_{O_2}, n_{N_2} are neutral concentrations, approximately calculated in accordance with a Boltzmann distribution, and the temperatures T_e, T_i, T_n are computed according to the analytical formulas $T(z) = T_{\infty} - (T_{\infty} - T_0) \exp\left(\frac{g}{RT_{\infty}}(z - z_0)\right)$ in good agreement with the experimental data. The constants in these formulas are taken as $T_{n\infty} = 800$ K, $T_{i\infty} = 950$ K, $T_{e\infty} = 2200$ K.

The first step is the change from the vector form of (2) to geographical coordinates in the assumption of a thin vertical layer (λ, φ, z) , where z is the altitude counted off from the Earth's radius a . In the considered coordinates the expression for the divergence is $\text{div}(n\vec{a}) = \frac{1}{a \cos \varphi} \left[\frac{\partial}{\partial \lambda}(na_x) + \frac{\partial}{\partial \varphi}(na_y \cos \varphi) \right] + \frac{\partial}{\partial z}(na_z)$, and the magnetic field components in the dipole approximations are $\vec{B} = (0, B \cos I, -B \sin I)$, where I is the magnetic inclination angle $I \approx \arctan(2 \tan \varphi)$.

In the considered coordinates equation (2) is given by

$$\frac{\partial n}{\partial t} = DYZ(n) + DTr(n) + Tr(n) + [P - kn], \quad (3)$$

where the terms in the right hand side are

$$Tr(n) = \frac{1}{a \cos \varphi} \frac{\partial}{\partial \lambda} \left[n \frac{1}{B} (E_y \sin I + E_z \cos I) \right] + \frac{1}{a \cos \varphi} \frac{\partial}{\partial \varphi} \left[\left(u_z \sin I \cos I - u_y \cos^2 I - \frac{E_x}{B} \sin I \right) n \cos \varphi \right] + \frac{\partial}{\partial z} \left[\left(u_y \cos I \sin I - u_z \sin^2 I - \frac{E_x}{B} \cos I \right) n \right]; \quad (4)$$

$$DYZ(n) = \frac{1}{a \cos \varphi} \frac{\partial}{\partial \varphi} \left(D \cos \varphi \left[\frac{1}{a} \frac{\partial n}{\partial \varphi} \cos^2 I - \frac{\partial n}{\partial z} \cos I \sin I \right] \right) + \frac{\partial}{\partial z} \left(D \left[\frac{\partial n}{\partial z} \sin^2 I - \frac{1}{a} \frac{\partial n}{\partial \varphi} \cos I \sin I \right] \right); \quad (5)$$

$$DTr(n) = \frac{1}{a \cos \varphi} \frac{\partial}{\partial \varphi} \left[\left(\frac{1}{a} \frac{1}{T_p} \frac{\partial T_p}{\partial \varphi} \cos^2 I - \frac{1}{T_p} \frac{\partial T_p}{\partial z} \cos I \sin I - \frac{1}{H} \sin I \cos I \right) Dn \cos \varphi \right] + \frac{\partial}{\partial z} \left[\left(-\frac{1}{a} \frac{1}{T_p} \frac{\partial T_p}{\partial \varphi} \cos I \sin I + \frac{1}{T_p} \frac{\partial T_p}{\partial z} \sin^2 I + \frac{1}{H} \sin^2 I \right) Dn \right]. \quad (6)$$

A detailed physical validation of the model and derivation of the equations are beyond this work and will be given in a separate article.

2.2. Properties of the differential problem

1. The model is based on a mass conservation law taking place in absence of sources and sinks, which means that the problem has a corresponding conservation principle.
2. According to its physical sense the solution of the equation is non-negative (since the initial conditions are always chosen to be non-negative).
3. Near the lower boundary the diffusion component and transfer are negligible with respect to the photochemistry processes. In contrast, at the upper boundary the diffusion processes are dominating, and photochemistry plays no role. An important characteristic of the problem is a great variation of the parameters D, P, k, u in the considered region (by several orders of magnitude) [13]. The characteristic times of different physical processes vary considerably, and this causes a strong stiffness in the problem.

3. Solution method and numerical modeling

Consideration of the problem properties, listed in the previous section, provides the following requirements on the finite-difference schemes:

1. In order to reproduce the mass conservation law, only conservative finite difference schemes must be used.
2. The non-negativity of the solution determines a necessity to use monotone schemes (in the sense of Godunov's definition).
3. Since the overall goal is to build a coupled thermosphere-ionosphere INM RAS model [1], it creates a requirement to use big time steps in order to reduce the computational load.
4. Since the equation is stiff, it is necessary to use implicit time discretization schemes (taking into account the previous requirement).

3.1. Splitting method

The main method used in this work is a splitting method. Specificity of our approach lies in the fact that in order to simplify the numerical solving procedure of the 3D equation (3) splitting is used with respect to the physical processes and the geometric variables. For this, in equation (3) major physical processes (forming the concentrations and velocity fields), a vertical direction (connected with the gravitation field), and a meridional direction (connected with the magnetic field in the mentioned approximation) are chosen. In this work, only photochemistry processes and diffusion transfer are considered (the first two terms and the last one in equation (2)). The first splitting step describes plasma-chemical processes and diffusion in a projection on the z -axis:

$$\frac{\partial n}{\partial t} = \frac{\partial}{\partial z} \left[D \sin^2 I \left(\frac{\partial n}{\partial z} + \left(\frac{1}{T_p} \frac{\partial T_p}{\partial z} + \frac{1}{H} \right) n \right) - \frac{1}{a} D \sin I \cos I \left(\frac{\partial n}{\partial \varphi} + \frac{1}{T_p} \frac{\partial T_p}{\partial \varphi} n \right) \right] + [P - kn]. \quad (7)$$

At the second splitting step, an equation describing diffusion along the meridional direction is solved:

$$\begin{aligned} \frac{\partial n}{\partial t} = & \frac{1}{a^2 \cos \varphi} \frac{\partial}{\partial \varphi} \left[D \cos^2 I \frac{\partial n}{\partial \varphi} \cos \varphi \right] - \frac{1}{a \cos \varphi} \frac{\partial}{\partial \varphi} \left[D \sin I \cos I \frac{\partial n}{\partial z} \cos \varphi \right] + \\ & + \frac{\partial}{\partial \varphi} \left[\left(\frac{1}{a} D \cos^2 I \frac{1}{T_p} \frac{\partial T_p}{\partial \varphi} - D \sin I \cos I \left(\frac{1}{T_p} \frac{\partial T_p}{\partial z} + \frac{1}{H} \right) \right) n \cos \varphi \right], \end{aligned} \quad (8)$$

As a result of the two splitting steps, equation (3) is solved in 2D approximation without neutral and transversal transfer:

$$\frac{\partial n}{\partial t} = DYZ(n) + DTr(n) + [P - kn]. \quad (9)$$

The third splitting step governs 3D transfer, $Tr(n)$.

3.2. Implementation of the first splitting step

In this work, the results of numerical modeling of only the first splitting step are presented. This approximate formulation has a physical sense in the middle latitudes and near the poles without perturbations [13]. Solving the problem at the first splitting step is performed in several approximate settings. In the first setting, a 1D equation including plasma chemistry and diffusion along z is considered:

$$\frac{\partial n}{\partial t} = P - kn + \frac{\partial}{\partial z} \left[D \left(\frac{\partial n}{\partial z} + \left(\frac{1}{T_p} \frac{\partial T_p}{\partial z} + \frac{m_i g}{2kT_p} \right) n \right) \right] \quad (10)$$

with a Dirichlet boundary condition $n_{z=z_b} = \frac{P(z=z_b)}{k(z=z_b)}$ at the lower boundary $z = z_b$ and a constant flux condition $D \left(\frac{\partial n}{\partial z} + \left(\frac{1}{T_p} \frac{\partial T_p}{\partial z} + \frac{m_i g}{2kT_p} \right) n \right) = F$ at the upper boundary $z = z_t$ (in this work, for simplicity the constant F is approximately taken 0).

In the next approximate setting, the latitudinal dependency is taken into account by considering a projection on the z -axis (in this case the diffusion coefficient gets a multiplier $\sin^2 I$):

$$\frac{\partial n}{\partial t} = P - kn + \frac{\partial}{\partial z} \left[D \sin^2 I \left(\frac{\partial n}{\partial z} + \left(\frac{1}{T_p} \frac{\partial T_p}{\partial z} + \frac{m_i g}{2kT_p} \right) n \right) \right]. \quad (11)$$

The third approximate setting takes into account the latitudinal dependency, which leads to the 2D equation (7).

In this investigation, all external parameters of the model (neutral concentrations, temperatures, etc.) are defined with empirical formulas (see Appendixes in [13]).

3.3. Approximation method

The main approximation method in this work is a finite difference method. We now consider spatial approximations of each term in the approximation settings (7), (10), (11). At point $z = z_i$ for the diffusion component $\frac{\partial}{\partial z} D \frac{\partial n}{\partial z}$ the following standard conservative second order approximation is used:

$$\frac{\partial}{\partial z} D \frac{\partial n}{\partial z} \approx \frac{D_{i+1/2}(n_{i+1} - n_i)}{h^2} - \frac{D_{i-1/2}(n_i - n_{i-1})}{h^2}. \quad (12)$$

Let $u = D \left(\frac{1}{T_p} \frac{\partial T_p}{\partial z} + \frac{m_i g}{2kT_p} \right)$ denote an effective velocity. Then $\frac{\partial}{\partial z} \left(D \left(\frac{1}{T_p} \frac{\partial T_p}{\partial z} + \frac{m_i g}{2kT_p} \right) n \right)$ can be simply written as $\frac{\partial}{\partial z} (n \cdot u)$. For this component, central difference and directed difference schemes are used. The lower boundary condition is approximated exactly, and the upper boundary condition is approximated consistently with the whole finite difference scheme.

The schemes mentioned above are used in numerical implementation of the 1D equation (10). We have shown that these schemes are conservative and the directed difference scheme is monotone in the hyperbolic component. The basic idea of the conservation proof is considering a finite-dimensional analogue of the integral of the electron concentration over the whole area, calculated with corresponding quadratures and showing that its time derivative is zero. For a proof of the scheme monotonicity it can be shown that the matrix of the finite-dimensional operator is an M -matrix, whence it follows that its inverse matrix has non-negative elements. Therefore, the solution holds its sign passing to the next time layer.

For equation (11) with the projection on the magnetic field lines (by adding a factor $\sin^2 I$), the same finite difference schemes are used with latitude φ added as an external parameter.

For the equation with a projection and a mixed derivative (7), the main idea for building finite difference schemes is based on representing the mixed derivative in the following form:

$$\frac{\partial}{\partial z} \frac{\partial n}{\partial \varphi} = \frac{\partial}{\partial z} \left(n \frac{1}{n} \frac{\partial n}{\partial \varphi} \right) = \frac{\partial}{\partial z} \left(n \frac{\partial \ln n}{\partial \varphi} \right). \quad (13)$$

We denote

$$u_\varphi = \frac{\partial \ln n}{\partial \varphi} = \frac{1}{n} \frac{\partial n}{\partial \varphi}. \quad (14)$$

For equation (7) u_φ is an additive to the effective velocity u corresponding to the mixed derivative. Formally, the linear mixed derivative is represented as a divergence transfer with an effective velocity depending on the solution. This velocity, u_φ , can be calculated explicitly with the following finite difference schemes:

1. The first method is approximating the derivative of $\ln n$ by φ with central or directed difference in φ . For the central difference scheme this approximation is

$$u_\varphi \approx \frac{\ln n_i^j(\varphi + \Delta\varphi) - \ln n_i^j(\varphi - \Delta\varphi)}{2\Delta\varphi}; \quad (15)$$

2. The second method is approximating this derivative without the \ln function:

$$u_\varphi \approx \frac{2}{n^j(\varphi + \Delta\varphi) + n^j(\varphi - \Delta\varphi)} \cdot \frac{n^j(\varphi + \Delta\varphi) - n^j(\varphi - \Delta\varphi)}{2\Delta\varphi}. \quad (16)$$

To approximate the mixed derivative term $\frac{\partial}{\partial z} (u_\varphi n)$ in z , two conservative schemes of the form $\frac{1}{h} (\Phi_{i+1/2} - \Phi_{i-1/2})$ are explored:

1. Central difference approximation:

$$\Phi_{i+1/2} = \frac{u_{\varphi(i+1)}n_{i+1} + u_{\varphi(i)}n_i}{2}; \quad (17)$$

2. Directed difference approximation with a flux calculated with

$$\Phi_{i+1/2} = \frac{u_{\varphi(i+1/2)} + |u_{\varphi(i+1/2)}|}{2h}n_i + \frac{u_{\varphi(i+1/2)} - |u_{\varphi(i+1/2)}|}{2h}n_{i+1}. \quad (18)$$

In numerical modeling of all considered approximation settings implicit time discretization schemes are used, according to the above-mentioned requirement on the computational efficiency of the solving methods. In this case the time step corresponds to the time step used in the INM RAS thermosphere model (1-5 minutes). The mixed derivative term is approximated with an explicit-implicit scheme: the effective additive u_{φ} that contains a latitudinal derivative is calculated with an explicit scheme, and the full term is approximated with an implicit one.

In the above-considered assumptions for computing the solution at the first splitting step, the following boundary conditions are used: at the lower z -boundary we have a Dirichlet boundary condition $n(z_b) = \frac{P(z_b)}{k(z_b)}$, and at the upper boundary, as before, the boundary condition is a constant flux, but this time with the addition of u_{φ} .

4. Results

We now proceed to the results of numerical experiments for the first version of the model in different approximation settings and their comparison. A detailed investigation is provided for convergence of the numerical solution to a stationary distribution in case of fixed daytime photoionization P . The spatial characteristics of the stationary solution of the finite difference problem within implementation of the finite difference schemes for the three main approximation settings (10, 11, 7) are also considered.

The numerical experiments in the approximation settings (10, 11) were performed with a space step $h = 5$ km and a time step $\tau = 3$ min. These values fit the properties of the INM RAS thermosphere model [1]. As for equations (11, 7), a latitudinal step of 1° was used.

The numerical experiments in settings without the mixed derivative (10, 11) have shown convergence to a stationary distribution that is close to the observed unperturbed electron concentration distribution in the terrestrial F layer in the middle latitudes [13]. The characteristic stabilization time has an order of 4 – 5 hours. Using various finite difference schemes for the hyperbolic part did not lead to a significant change in the results.

A comparison of the results of the numerical experiments on the reconstitution of a daytime stationary vertical distribution for the main approximation settings (10, 11, 7) in different latitudes is given in Figure 1. It can be easily seen that the largest differences (as it follows immediately from the equations) are observed near the equator, whereas the closest solution to the characteristic distribution in the terrestrial ionosphere in this case is obtained from equation (10).

A distinctive feature of equations (11) and (7) (taking into account the inconsistency of the vertical and magnetic field directions) is a singular non-physical photochemistry solution at the equator: $n = \frac{P}{k}$. As a consequence, near the equator the solution has a significant latitudinal gradient. Numerical experiments on solving (7) with the mixed derivative have shown that the central difference scheme (15, 16) in φ gives an intense false two-step oscillation spreading from the equator with a rising amplitude. The implementation of the directed difference formula in φ , on the contrary, did not cause any significant problems. A remarkable fact is that there is

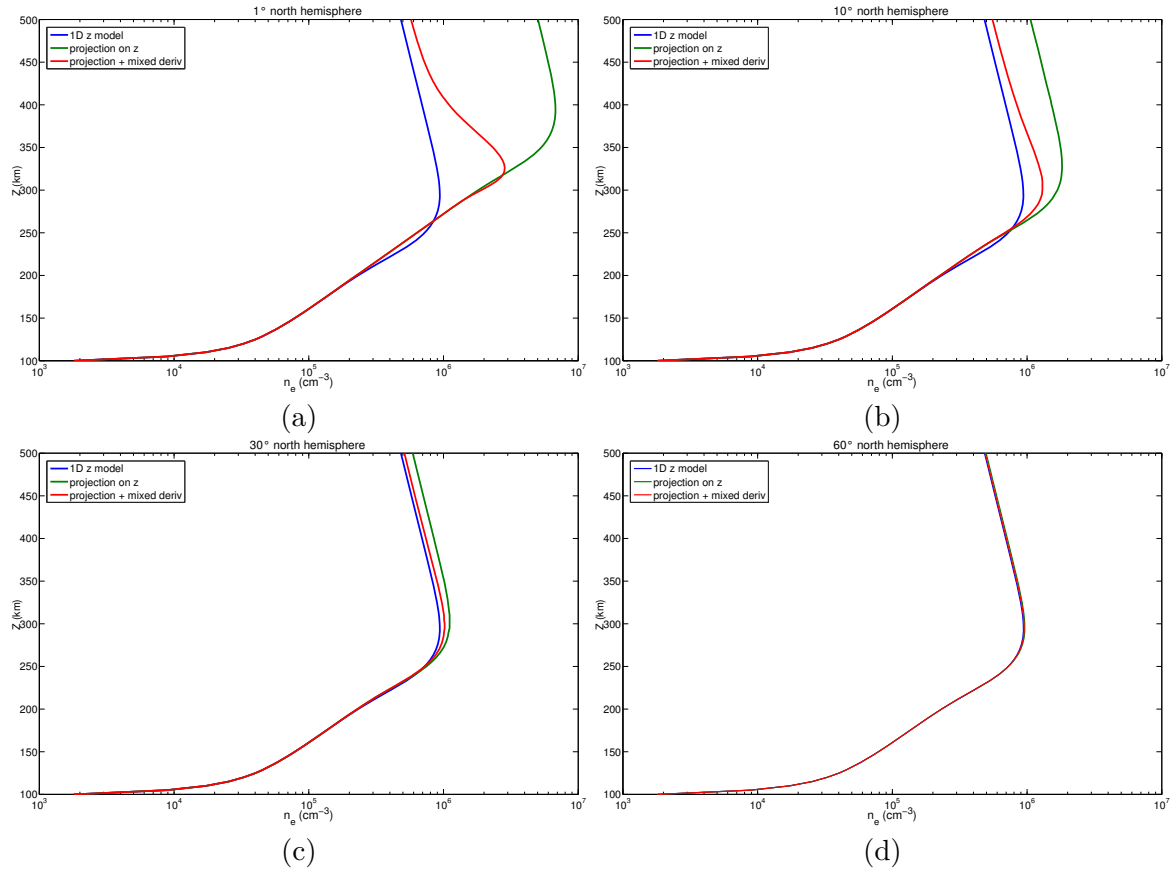


Figure 1. Vertical distributions of the electron concentration (cm^{-3} , in log scale) subsequent to the results from three approximation settings (blue — (10), green — (11), red — (7)) at different latitudes: (a) -1° , (b) -10° , (c) -30° , (d) -60° north latitude (for the south latitude the solution is the same according to the symmetry of the equation).

no observable difference between the approximations of u_φ with the logarithm and the simple directed difference (15, 16).

Figure 2 illustrates the results of calculating the height-latitudinal distributions in approximation settings without the mixed derivative term (11) and with this term (14) after the calculation for a day. It is easy to see that adding the mixed derivative component can have an impact not only near the equator, but also in subtropical zones up to the middle latitudes.

Despite limitations, the above-considered first version of the model gives a possibility to investigate the primary physical problem of sensitivity to parameters of the equation which are external for the ionosphere. Figure 3 shows the vertical electron concentration profiles for the 1D equation (10) with variation of the following parameters: $n_O(z_0)$ in Boltzmann distribution, temperatures $T_{n\infty}$ and $T_{e\infty}$ at the upper boundary of the considered area, and photoionization P . It was demonstrated that the profile has the highest sensitivity to the neutral temperature, the ionization level, and the atomic oxygen concentration. The other parameters have a slight impact on the solution. It is important to notice that the specific variability structure of n by virtue of the neutral temperature (mainly variation of the altitude of the F region maximum) is qualitatively different from the structure corresponding to the photoionization (variation of the maximum value of the F region). This result might be of importance for understanding the mechanisms of ionosphere variability.

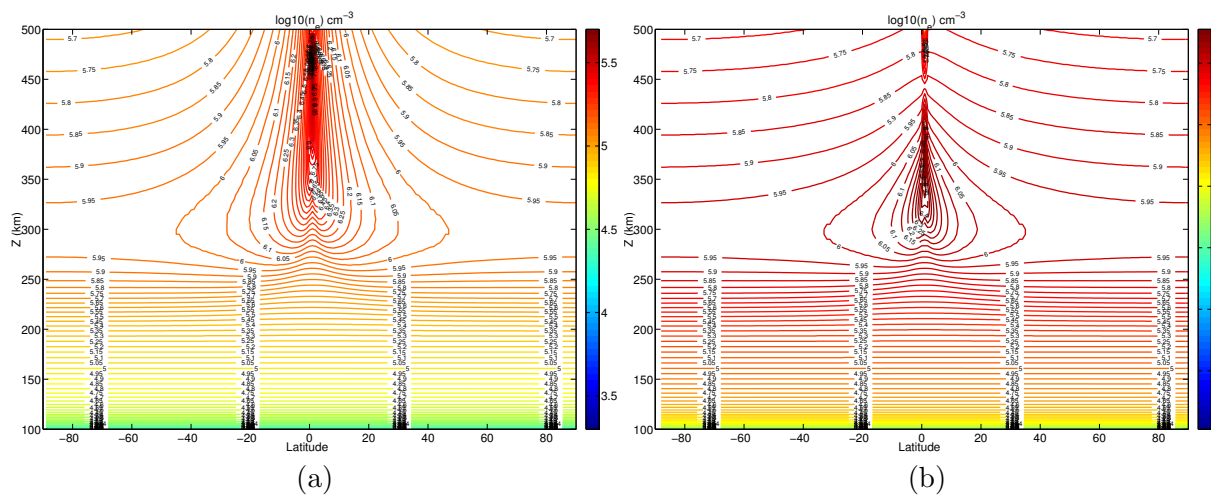


Figure 2. Height-latitudinal distributions of electron concentration (decimal logarithm, cm^{-3}) according to the results of the created ionosphere model in the approximation setting with vertical direction projection without the mixed derivative ((11) (a)) and with it ((7) (b)). Isolines are drawn with a step of 0.05.

5. Conclusions

In conclusion, we briefly outline the basic results.

A complete 3D model of the terrestrial ionosphere's F layer was stated and formulated in spherical layer coordinates. The model includes the main physical processes forming the ionosphere. An original method was suggested for a stage-by-stage realization of the model with splitting with respect to the physical processes and the geometric variables. The first splitting step for the vertical direction was implemented in three approximation settings (considering only the vertical diffusion, taking into account a projection on the magnetic field lines without or with a mixed derivative term). Several finite difference schemes were implemented: the diffusion part was approximated with a central difference scheme and for the hyperbolic transfer central and directed difference approximations were employed. The conservation and monotonicity were shown for a directed difference scheme for the first setting.

An essentially novel technique in the context of numerical methods was used in solving the equation with the mixed derivative. Several original ways of approximating this derivative were suggested. It was also shown that the central difference approximation along one of the directions can give significant numerical errors and is not recommended in case of expecting strong gradients of the solution.

Generally, an analysis of the obtained results has shown the applicability of the discussed approximation setting to modeling of the ionosphere's F layer in an unperturbed condition in the middle latitudes and the necessity to consider meridional diffusion in a region near the equator where the magnetic field is approximately horizontal. This consideration will be the first stage of future work.

Through the use of the dynamical model in the middle latitudes the sensitivities of the stationary electron concentration vertical distribution to external equation parameters were investigated. The most remarkable result (from a physical standpoint) is that the greatest relative influence on the concentration distribution has been exerted by the neutral temperature, atomic oxygen concentration, and ionization level. Therewith the spatial variability structures determined by the mentioned variations are qualitatively different.

According to the successful implementation of the first splitting step in the above-suggested scheme, a general strategy of solving the problems stated in the introduction includes stepwise

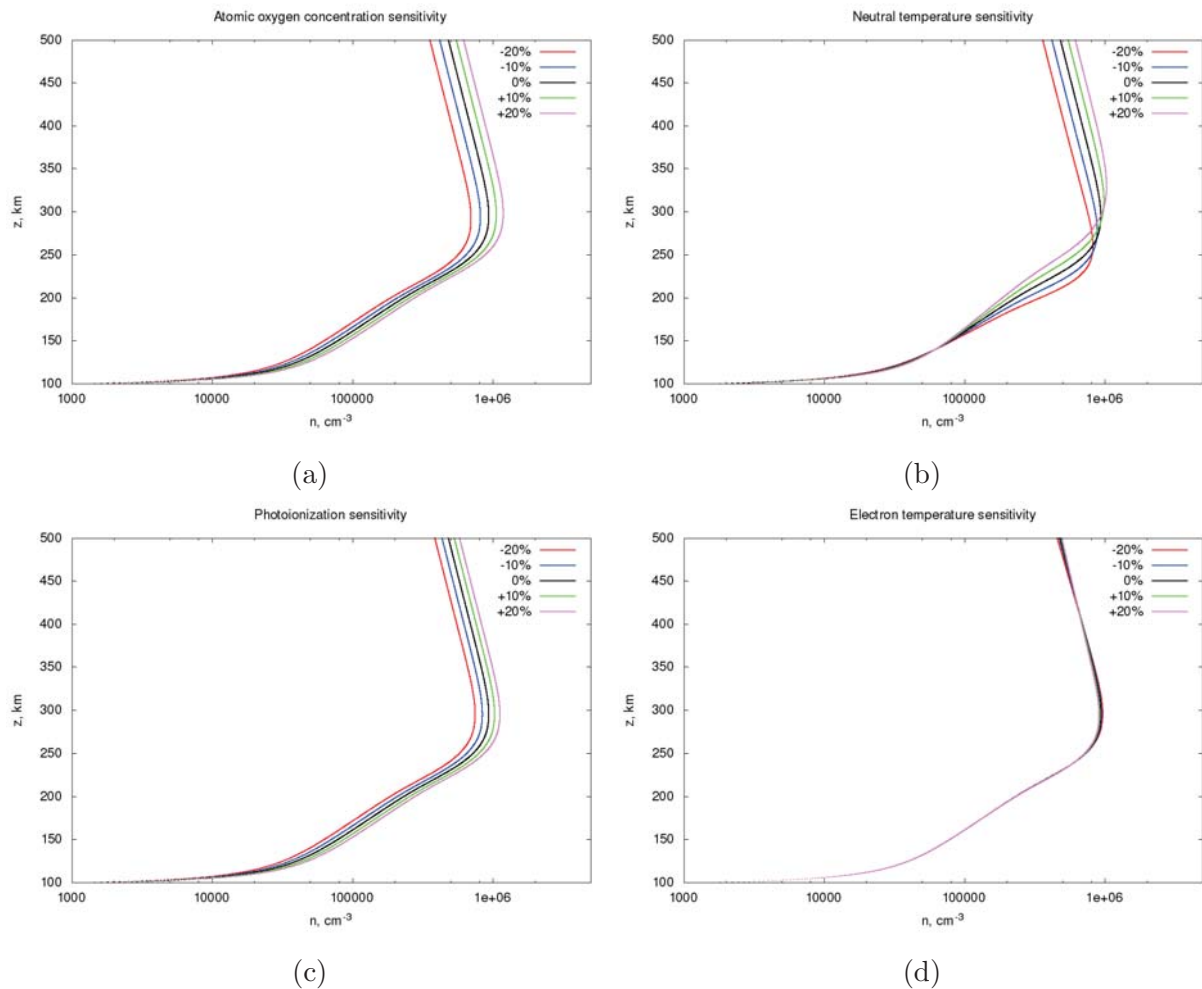


Figure 3. Electron concentration vertical distribution (cm^{-3} , in log scale) obtained by variation of the parameters external for the ionosphere model (10) by 10% and 20% on either side: (a) atomic oxygen concentration, (b) neutral temperature, (c) photoionization P , (d) electron temperature.

solving of the complete 3D equation based on the above-discussed algorithms and an integration of the model into a developed thermosphere's model.

Acknowledgments

The work was supported by Russian Science Foundation (project no. 17-17-01305).

6. References

- [1] Kulyamin D V and Dymnikov V P 2013 A three-dimensional model of general thermospheric circulation *Russian J. Numer. Anal. Math. Modelling* **28**(4) 353-80
- [2] Kulyamin D V and Dymnikov V P 2015 Modelling of the lower ionosphere climate. *Izv. - Atm. Ocean. Phys.* **51**(3) 272-91
- [3] Bilitza D, McKinnell L A, Reinisch B and Fuller-Rowell T 2011 The International Reference Ionosphere (IRI) today and in the future *J. Geodesy*, **85** 909-20
- [4] Leshchinskaya T Y, Mikhailov V V 2016 SIMP-1 model: mapping of fo F2 monthly medians over the Northern *Geomagnetism and Aeronomy* **56**(6) 733-41

- [5] GOST 25645.146-89 *The Earth's ionosphere. Model of global distribution of concentration, temperature, and effective collision rate of electrons* (Moscow: Izdatel'stvo standartov) 1990
- [6] Richmond A D, Ridley E C and Roble R G 1992 A Thermosphere/Ionosphere General Circulation Model with coupled electrodynamics *Geophys. Res. Lett.* **19** 601-4
- [7] Roble R G, Ridley E C, Richmond A D and Dickinson R E 1988 A coupled thermosphere/ionosphere general circulation model *Geophys. Res. Lett.* **15** 1325-8
- [8] Bailey G J, Balan N and Su Y Z 1997 The Sheffield university plasmasphere ionosphere model: a review *Journal of Atmospheric and Solar-Terrestrial physics* **59**(13) 1541-52
- [9] Namgaladze A A, Martynenko O V, Volkov M A, Namgaladze A N and Yurik R Yu 1998 High-latitude version of the global numerical model of the Earth's upper atmosphere *Proceedings of the MSTU*. **1**(2) 23-84
- [10] Surotkin V A, Klimenko V V and Namgaladze A A 1979 A numerical model of the equatorial ionosphere *Investigation of the ionospheric dynamics* 58-68
- [11] Schunk R W, Scherliess L, Sojka J J, Thompson D C, Anderson D N, Codrescu M, Minter C, Fuller-Rowell T J, Heelis R A, Hairston M and Howe B 2004 Global assimilation of ionospheric measurements (GAIM) *Radio Sci.* **39** RS1S02
- [12] Khattatov B, Murphy M, Gnedin M, Sheffell J, Adams J, Cruickshank B, Yudin V, Fuller-Rowell T and Retterer J 2005 Ionospheric nowcasting via assimilation of GPS measurements of ionospheric electron content in a global physics-based time-dependent model *Q. J. R. Meteorol. Soc.* **131** 3543-59
- [13] Schunk R W and Nagy A F 2009 *Ionospheres Physics, Plasma Physics, and Chemistry* (New York: Cambridge University Press)